Cascading photoinduced, elastic, and thermal switching of spin states triggered by a femtosecond laser pulse in an Fe(III) molecular crystal

M. Lorenc,[1,*] Ch. Balde,[1,†] W. Kaszub,[1,2] A. Tissot,[3] N. Moisan,[1] M. Servol,[1] M. Buron-Le Cointe,[1] H. Cailleau,[1] P. Chasle,[1] P. Czarnecki,[2] M. L. Boillot,[3] and E. Collet[1]

[1]*Institut de Physique de Rennes, UMR UR1-CNRS 6251, Université de Rennes1, Bat 11A–Campus de Beaulieu, F-35042 Rennes, Cedex, France*

[2]*Faculty of Physics, Adam Mickiewicz University, 85 Umultowska, Poznan 61-614, Poland*

[3]*Institut de Chimie Moléculaire et des Matériaux d'Orsay, UMR CNRS 8182, Université Paris-Sud 11, 91405 Orsay, France*

(Received 27 May 2011; revised manuscript received 12 January 2012; published 6 February 2012)

In this paper we put on solid ground the optical time-resolved study of spin-state photoinduced switching in an Fe(III) compound whose structural dynamics have been recently unveiled. We provide the experimental evidence of complex dynamics, occurring in succession, and spanning ten decades in time. We show that in addition to the ultrafast photoinduced molecular switching occurring on the subpicosecond timescale, there exists two additional switching processes significantly affecting the fate of the macroscopic material: one driven by elastic interactions as volume expansion occurs on a tens of nanoseconds timescale, and another one associated with heat diffusion and thermal switching taking place on a tens of microseconds timescale.

DOI: 10.1103/PhysRevB.85.054302 PACS number(s): 31.70.Ks, 42.70.Gi, 82.53.Xa, 78.47.−p

I. INTRODUCTION

The ability to control with an ultrashort laser pulse molecular state in a solid, and consequently its macroscopic properties, is regarded as one of the next major strides in material science. Contrary to dilute solutions, the crystal may be wholly constituted of switchable molecules thereby mediating self-amplification processes. This opens new avenues for light control of various photoinduced switchable functions (magnetic, optical, conduction. . .),[1–3] with possible direct consequences on future developments of information technologies. Spin-crossover compounds[4] promise bright perspectives owing to photoactivated molecular bistability between low spin (LS) and high spin (HS) states. In these compounds, Light-Induced Excited Spin State Trapping (LIESST) is stabilized through structural relaxation.[4] Cooperative response brought about in solids by elastic interactions between molecules enables efficient generation of HS states, which is exemplified by light-induced bistability to/from photostationary states at low temperature.[4–7] Despite reports on relaxation mechanisms after nanosecond laser excitation,[4,8–12] little has been known about the out-of-equilibrium dynamics of spin-crossover systems. Ultrafast measurements of such photoinduced switching have been mostly restricted to a single molecule in solution.[13–17]

We have recently reported[18] on the ultrafast spin-state photoinduced switching and the consecutive transformation dynamics in a catecholato-Fe(III) spin-crossover complex [(TPA)Fe(TCC)]PF_6 (TPA = tris(2-pyridylmethyl)-amine, H_2TCC = 3,4,5,6-tetrachlorocatecholate). Its monoclinic polymorph,[19] studied here, undergoes spin-crossover from a low temperature, LS ($S = 1/2$) state to a high temperature, HS ($S = 5/2$) state. This thermal conversion is centered at $T_{1/2} = 214$ K, where the HS molecular fraction $X_{HS} = 1/2$ [Fig. 1(a)]. The variation of X_{HS} drives significant changes of magnetic susceptibility ($\chi_m T$), optical properties, and intramolecular structure (mainly around the central Fe ion) of the compound. Time-resolved x-ray diffraction and femtosecond optical spectroscopy have demonstrated that the excitation of a single crystal by femtosecond laser flash can switch the molecular state from LS to HS, whereby different processes and timescales are involved during the out-of-equilibrium dynamics. These dynamics span vast timescales from subpicosecond nonthermal molecular transformation to slower thermal switching and diffusive heating through the lattice on the microsecond timescale. That study[18] relied on combining the time-resolved x-ray diffraction with ultrafast laser spectroscopy and permitted laying ground for the interpretation of the out-of-equilibrium spin-crossover dynamics, including the equilibrium recovery. According to our current understanding of the spin-crossover, the structure and the electronic properties depend directly on the spin state of the metal ion and so should concurrently follow the spin-state dynamics.

The bottom line of the present study was to cover several decades of time in one experiment, whereby a femtosecond laser pulse initiates an electronic transition, and a second delayed laser pulse monitors the transient absorbance of the crystal. By relying on two different gating schemes for probing the time evolution of the material response to light excitation while utilizing the same laser source, we were able to cover ten time decades beginning with femtosecond Franck-Condon (FC) excitation and ending with millisecond relaxation.

The paper is organized as follows. In Sec. II we describe the experimental procedure, and, in particular, the new set-up allowing the extension of spectroscopically observable timescales, while preserving the excitation conditions in the entire time window. Sec. III is a comprehensive analysis of the new optical data obtained and to our knowledge never followed over so many time decades at once, in keeping with the structural dynamics.[18] In Sec. IV we provide a phenomenological account of the different dynamical steps observed. In particular, the proposed quantitative description of time-resolved thermal conversion is further supported by independent calorimetric measurements.

 ©2012 American Physical Society

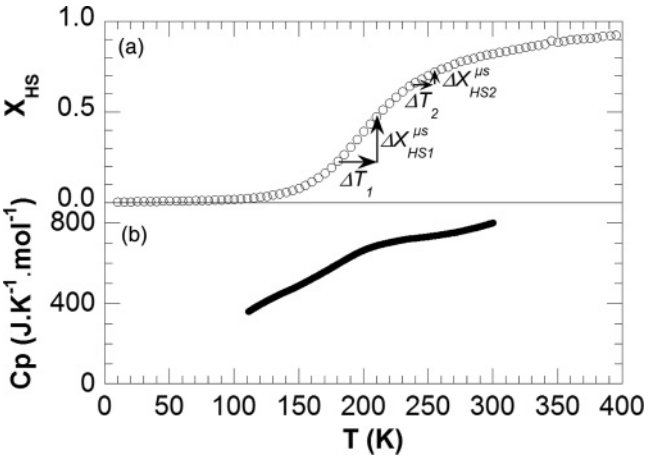

FIG. 1. (a) Fraction of molecules in high spin state during thermal crossover, as extracted from magnetic susceptibility measurements (from Ref. 19). (b) Temperature dependence of heat capacity measured with DSC on a bulk sample. Sketched with arrows: temperature increase ΔT_1 and ΔT_2 induced at T_1 and T_2 with the same laser energy and the resulting thermal conversion of HS fraction, $\Delta X_{\mathrm{HS1}}{}^{\mu s} > \Delta X_{\mathrm{HS2}}{}^{\mu s}$.

II. EXPERIMENTAL

A. Stationary magnetic studies

The single crystals of the monoclinic polymorph of [(TPA)Fe(TCC)]PF_6 were characterized earlier by magnetic susceptibility, optical, and x-ray diffraction measurements.[19] As both HS and LS states are magnetic, the measured $\chi_m T$ product of molar magnetic susceptibility χ_m and temperature T, is a sum over fractions of pure HS (X_{HS}) and pure LS ($1 - X_{\mathrm{HS}}$) states, changing with T according to

$$\chi_m T = X_{\mathrm{HS}}(T) \times (\chi_m T)_{\mathrm{HS}} + (1 - X_{\mathrm{HS}}(T)) \times (\chi_m T)_{\mathrm{LS}}. \quad (1)$$

From the $\chi_m T$ product, obtained with SQUID measurement, the temperature dependence of X_{HS} can be extracted, and as such is given in Fig. 1(a). It is typical of a gradual thermal spin-crossover from the high temperature, HS state to the low temperature, LS state. The characteristic temperature at which $X_{\mathrm{HS}} = 1/2$ is equal to 214 K.

B. Differential scanning calorimetry studies

Differential scanning calorimetry (DSC) was performed with a Thermal Analysis Q2000 type calorimeter in the temperature range from 100 K to 300 K and at different heating rates from 2 to 10 K/min. Small single crystals were used for those measurements. The temperature dependence of heat capacity shown in Fig. 1(b) reveals a broad anomaly, beginning at 140 K and terminating at 280 K with midpoint at 214 K. The temperature scan starts at $X_{\mathrm{HS}} \approx 0$ and stops at $X_{\mathrm{HS}} \approx 1$. The anomaly shows a hump centered around $T_{1/2}$. Therefore, the observed anomaly in heat capacity, reminiscent of weakly cooperative systems,[20] has to be due to the spin-crossover.

C. Time-resolved optical study

Time-resolved optical measurements were performed with pump-probe method on single crystals of [(TPA)Fe(TCC)]PF_6 (Fig. 2). Crystals were excited at 800 nm and probed at 600 nm, the latter wavelength being identified as most sensitive to the spin-crossover in the visible (VIS) range.[18] The excitation was provided from the direct output of a femtosecond regenerative amplifier (Legend USP, Coherent). The probe light was generated by another femtosecond regenerative amplifier (Legend Elite, Coherent) followed by an optical parametric amplifier (TOPAS, Light Conversion) to allow tuning the probe wavelength. The pump-probe cross-correlation measured in a separate experiment was found equal to 110 fs. The crystals were plate shaped and selected such that their size, typically 200 × 150 μm^2, left no clear aperture for the probing light. The experiments were configured in transmission geometry. The two laser beams, pump, and probe, intersect at a 7° angle on the crystal, with the probe beam propagating parallel to the crystal axis b. Both pump and probe were polarized parallel to the long crystal axis a, along which the laser penetrates deepest.[19] Typically the crystals were 5–10-μm thick, thus setting the optical density (OD) for VIS probing light to a value within 1–1.5 at 100 K (LS state). This thickness strikes good compromise between laser penetration length (3–5 μm at 800 nm) and the number of

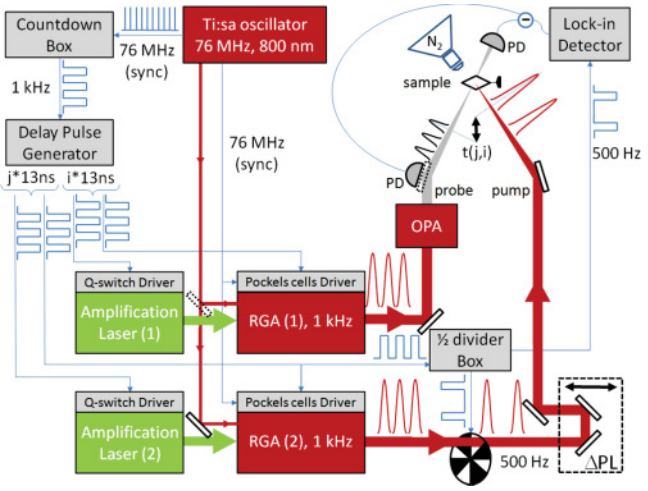

FIG. 2. (Color online) The timing set-up and the optical layout of the time-resolved pump-probe experiment. The thin lines show schematically the connections between different instruments synchronized to the trigger signals delivered by the delay pulse generator. The electronic trigger signals of different frequencies and phases are drawn for clarity. The delay pulse generator sets the desired timing pattern for the four lasers: amplification lasers (1) and (2) and the regenerative amplifiers RGA(1) and RGA(2). Any pump-probe delay, $t(j, i)$, being a multiple number of 13 ns (inverse of $f_{\mathrm{RF}} = 76$ MHz) is thereby generated. Shorter pump-probe delays, from 100 fs to 1 ns, are attained by adjusting the optical path difference (ΔPL) with a mechanical translation stage. The thick lines represent the laser beams as they propagate from the sources to the sample. The laser beams are polarized parallel to the crystalline axis a. The sample is cooled with nitrogen flow (N_2). The transmitted laser light is detected with two balanced photodiodes. The phase and intensity of the differential signals are recorded with a lock-in amplifier.

excited molecules in the probed bulk. The temperature of the crystals was maintained with nitrogen gas flow (Oxford Instruments).

The laser set-up (Fig. 2) requires that several sources operate in synchrony: the femtosecond oscillator (Ti:sa), the amplification pump lasers [Laser(1) and Laser(2)] used to power the amplification stages, and the regenerative amplifiers [RGA(1) and RGA(2)]. The timing between these optical components is handled by the digital synchronization electronics. Every laser pulse from the Ti:sa oscillator is split in two by a beam splitter, thereby providing pump and probe twinned pairs with zero temporal jitter. These pulses are trapped and amplified by the regenerative amplifiers which operate at 1 kHz each. Because of a mismatch between operating frequencies of the "free-running" oscillator and the amplifiers, the relative timing will vary in time and will have an upper limit equal to the interpulse spacing of the oscillator. To overcome this limit, the reference signal given by the repetition rate of the oscillator (Mira Seed, Coherent) is divided down to 1 kHz (programmable countdown box, Coherent), and this new frequency is fed to a 4 channel digital-delay pulse generator (DDPG, model 9524 Quantum Composers) delivering phase-locked trigger signals at 1 kHz to two regenerative amplifiers RGA(1) and RGA(2). Each amplifier requires two such signals, one for Q-switching the amplification laser and one for triggering the regenerative amplifier switches, the so-called Pockels cells. These cells are responsible for trapping only one pulse from the radio-frequency (RF) train for amplification, and a timing mismatch of barely 1–2 ns could result in multiple pulse output. Therefore, the phase of 1 kHz signal triggering the Pockels cells is additionally compared to the reference (sync) signal by fast electronics (SDG, Coherent). The operation principle of regenerative amplifiers has not changed since it was first demonstrated in the 1980s. Here we simply operate two such amplifiers in synchrony. It results in a slightly more elaborate scheme whereby the delay generator sets the desired timing pattern. For example, by delaying the Pockels cells of the RGA(1) and the Q-switch driver of its amplification Laser(1), a later pulse from the RF train is trapped and amplified with respect to that trapped in the RGA(2). Owing to the common time origin, the pulses from the RF train can be electronically enumerated by the delay generator. If i and j were to tag the pulses from RGAs (1) and (2), respectively, the pulses can be fired at well-defined instants:

$$t_1(i) = PL_1 + t(0)_1 + i/f_{\mathrm{RF}} \quad (2)$$

$$t_2(j) = PL_2 + t(0)_2 + j/f_{\mathrm{RF}}, \quad (3)$$

where $f_{\mathrm{RF}} = 76$ MHz, $t(0)$ is the time offset for gating DDPG channels, and PL_1 and PL_2 define the optical path length from RGAs (1) and (2) to the sample. Because the time offset is constant during the gating process the variable delay between gated pulses is expressed directly from Eqs. (2) and (3) as

$$t(j,i) = \Delta PL + (j - i)/f_{\mathrm{RF}}, \quad (4)$$

where $\Delta PL = (PL_2 - PL_1)$. It is straightforward from Eq. (4) that any delay being a multiple number of 13 ns (inverse of 76 MHz) can be generated by electronically gating two amplifiers.

Shorter delays were monitored using a conventional scheme described earlier.[21] The time gating is essentially based on setting the optical path difference, $\Delta PL = t \times c$ (c being light velocity in air), between pump and probe by means of a mechanical translation stage. By combining both schemes on the same experiment, we can monitor the dynamical response to a laser excitation from 100 fs to 1 ms under constant excitation conditions.

Phase-sensitive detection is used for measuring pump-probe dynamics.[22] Briefly, the probe signal at the detector (Stanford Research System, SR830) was balanced against the reference signal to null the background at 1 kHz. The frequency of the pump is divided to 500 Hz with an optical chopper phase-locked to the laser. Synchronous modulation prevents phase drift between pump and chopper, whereas synchronous detection at the pump frequency ensures that only the difference component of the probe signal is amplified.

III. RESULTS FROM TIME-RESOLVED OPTICAL STUDY

We used excitation densities of up to 100 μJ/mm^2; below the damage threshold we found 300 μJ/mm^2. During the thermal crossover, between 90 K and 300 K, the transmission at 600 nm increases by a factor of approximately 3.[18,19] The optical pump-probe experiment was performed at 200 K, where the fractions of HS and LS molecules are close to 0.5 each. The experimental observables in these measurements are $\Delta I(t)$ and I, differential intensity and absolute intensity of transmitted probe light, respectively. The differential intensity is a difference of intensity between transmitted probe pulses in the presence and in the absence of the pump pulse. Figure 3(a) shows real-time data for 40 μJ/mm^2 excitation density ($\approx$2 photons/100 molecules in the bulk crystal), where three steps can be clearly identified. Namely, the first step is the

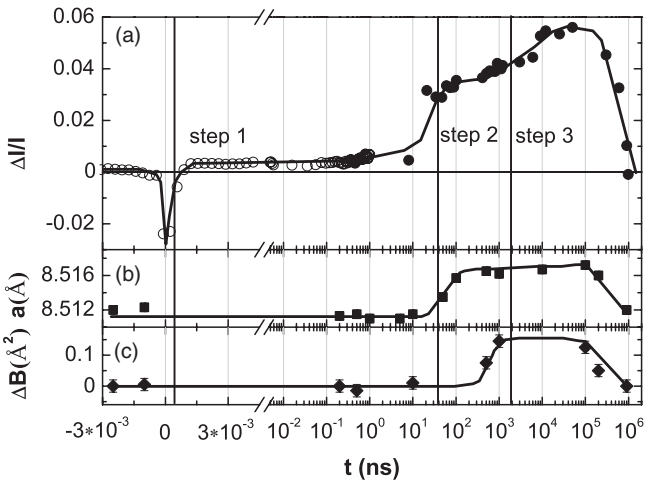

FIG. 3. (a) Differential intensity of transmitted probe light ($\Delta I/I$) measured on a single crystal of [(TPA)Fe(TCC)]PF_6 at 200 K by femtosecond excitation at 800 nm and 4 μJ/pulse with probe at 600 nm, obtained with 110 fs time resolution inside 1 ns time window (open circles) and obtained by electronically gating two synchronized femtosecond lasers (full circles). (b), (c) Time-resolved x-ray diffraction experimental data taken from Ref. 18: lattice parameter a (b) and variation of Debye-Waller factor B between $t < 0$ and $t > 0$ (c). Solid lines are drawn to guide the eye.

femtosecond photoinduced switching between molecular LS and HS states. This step proceeds through ultra-fast population of Ligand-to-Metal Charge-Transfer (LMCT) state(s) that the observed transient peak corresponds to, followed by a molecular relaxation populating HS state, which shows through a long-lived increase of optical transmission. The second step, associated with an even bigger variation of optical transmission, occurs on a tens of nanoseconds timescale. This is the relevant timescale for the volume expansion[18] and will be hereafter referred to as elastic step. The third step, associated with an additional variation of optical transmission, occurs on a tens of microsecond timescale when heating effects set in,[18] and thus will be referred to as thermal step.

A. Femtosecond photoinduced switching step

A transient absorption peak due to the LMCT state,[18] appearing within experimental resolution, is followed by the increase of transmitted intensity of the probing light [Fig. 3(a)]. This signature has been associated with the exponential population of the HS state from the LMCT state, however, a more complicated cascading relaxation cannot be excluded from the primary relaxation scheme. LMCT vanishes with a time constant of 300 fs, which is in very good agreement with timescales reported for spin-crossover molecules in solution,[13–17] as well as for the orthorhombic polymorph of the present material.[21] The molecules photoconverted to the HS state constitute a fraction ΔX_{HS} of all molecules in the crystal, and this fraction can be estimated according to

$$\Delta X_{\mathrm{HS}} = \frac{\Delta OD(t)}{\Delta OD}, \tag{5}$$

where

$$\Delta OD(t) = -\log\left(\frac{\Delta I(t)}{I} + 1\right) \tag{6}$$

is the OD variation after laser excitation at a given time t, and ΔOD is the variation between OD at 10 K ($X_{\mathrm{HS}} = 0$), and OD at 400 K ($X_{\mathrm{HS}} = 1$). From the data on the femtosecond timescale we can deduce that $\Delta X_{\mathrm{HS}}{}^{\mathrm{fs}}$ reaches ≈0.007 and remains unchanged over to 1–10 ns [Fig. 3(a)]. Time-resolved diffraction studies have demonstrated that this process occurs at constant crystalline volume.[18]

B. Nanosecond elastic step

Time-resolved x-ray diffraction revealed that volume expansion takes place at ≈50 ns,[18] as shown in Fig. 3(b). During this elastic step we can observe that the transmission increases again [$\Delta I/I$ between −3 ps and 100 ns, Fig. 3(a)] and does so to a significantly higher level than upon photoinduced switching at the first step. It can be inferred from Eq. (5) that this increase, associated with an increasing number of HS molecules, results in a higher fraction of converted HS molecules at the nanosecond step $\Delta X_{\mathrm{HS}}{}^{\mathrm{ns}} \approx 0.042$. In a recent report[23] where this mechanism was investigated by time-resolved x-ray diffraction, such an increase of HS molecules between 1 ns–100 ns was barely evidenced. This is the first time we observe this feature so clearly, which we attribute to an excellent signal-to-noise ratio of the lock-in detection.

The intensity of transmitted light is affected by the number of HS molecules in the laser-probed volume, hence the density of HS molecules rather than their absolute number describes the optical observable most accurately. The laser beam cross-section on the sample does not vary during the measurements, as opposed to the crystalline volume which expands upon spin-crossover. As a result, certain molecules leave the area delimited by the beam cross-section, thus affecting $\Delta I(t)$. The ratio between the number of molecules in the volume probed along b, prior to and after the expansion, equals the ratio between the unit cell surfaces $(a \times c)/(a' \times c')$ perpendicular to b; cell parameters of the expanded unit cell being primed for clarity. Between $t < 0$ and 100 ns a changes from 8.511 Å to 8.516 Å and c changes from 9.266 Å to 9.270 Å,[23] and even though b changes too, its contribution cancels out when the laser beam propagates parallel to b. With all of this factored in, the ratio $(a \times c)/(a' \times c')$ has the value ≈0.001. Given the magnitude of $\Delta X_{\mathrm{HS}}{}^{\mathrm{ns}}$ observed at 100 ns, that is ≈0.042, the latter increase cannot be explained solely by the change of HS density following volume expansion. Rather, the change observed at 100 ns is mainly associated with an additional conversion from LS to HS states, whose mechanism must be of elastic origin.

C. Microsecond thermal step

According to Fig. 3(a) the optical transmission increases again on the microsecond timescale. This slow evolution was demonstrated, by following the time dependence of the Debye-Waller[18] factor, to be related to the heat diffusion through the sample. The temperature homogenization leads to an increase of the average temperature, experimentally observed through increase of the Debye-Waller factor, ΔB between $t < 0$ and $t > 0$ Fig. 3(c). Indeed, the optical energy (≈1.55 eV) applied to switch the states from LS to HS is much higher than the energy difference between these states (tens of millielectron volts), and the nonradiative relaxation generates heat rapidly dissipating over the lattice vibrational modes. Besides, the finite penetration depth of the pump pulse causes gradients of local temperature, and the temperature homogeneity in the crystal is restored only on a microsecond timescale. The resulting heating drives the thermal population of HS state.[18] From the amplitude of the signal at 1–10 μs observed in Fig. 3(a), we can conclude that the HS fraction at the microsecond step, $\Delta X_{\mathrm{HS}}{}^{\mu\mathrm{s}}$, reaches ≈0.09 at 200 K.

D. Relaxation dynamics

The last feature observed in Fig. 3(a) is the HS relaxation, within approximately 1 ms. This is in agreement with the previously reported structural study as well as the measurements of optical reflectance.[18] The latter, however, was inherently sensitive to the changes on crystal surface only, and the time resolution was limited by the integration time as long as 100 μs. The photoinduced processes and the relaxation are no longer time-averaged in the present optical study, where a distinct stepwise spin-switching precedes the relaxation. Besides, the optical transmission rather than reflectivity can in principle probe propagation and diffusion processes in all three dimensions of the crystal.

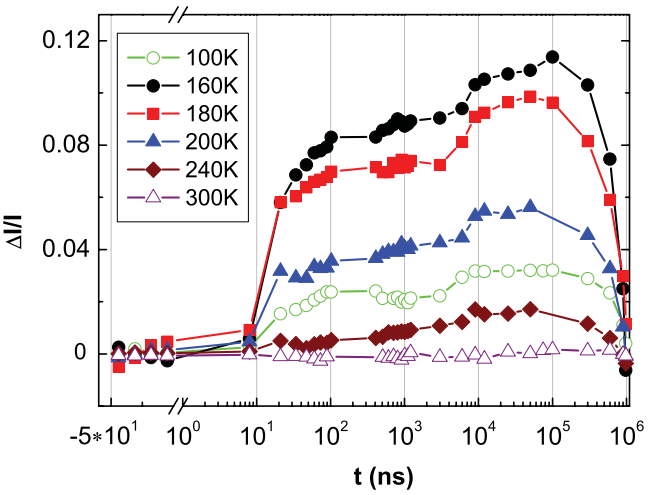

FIG. 4. (Color online) Time-resolved differential intensity of light transmitted by the crystal ($\Delta I/I$) from -50 ns to 1 ms at different temperatures; pump and probe as described in Fig. 3(a). Symbols are experimental data points. Solid lines are drawn to guide the eye.

E. Temperature dependence

Time-resolved differential intensity of light transmitted by the crystal, ($\Delta I/I$), from -50 ns to 1 ms at different temperatures is shown in Fig. 4. The sudden increase of transmission associated with lattice expansion is clear at all temperatures and occurs within ≈50 ns following excitation. The present method based on pulse selecting provides time-scan intervals of ≈13 ns, which still precludes accumulating several time delays between 1 ns (end of translation stage) and 13 ns. Despite this limitation, $\Delta I/I$ shows clearly an overall increase throughout the investigated time domain. When temperature is increased from 100 K to 160 K, $\Delta I/I$ grows. From that point, when temperature is increased to 180 K and above, $\Delta I/I$ diminishes. This behavior contrasts with the ultrafast dynamics, whose temperature dependence of $\Delta X_{\mathrm{HS}}{}^{fs}(T)$ exhibits gradual decrease with temperature rising Fig. 5(a).

The thermal step is observed too, with its maximum appearing at ≈100 μs, irrespective of temperature. This is more detailed in Fig. 5(b), which shows the amplitude of the signal measured at 100 μs and converted with Eq. (5) to $\Delta X_{\mathrm{HS}}{}^{\mu s}$. This thermal conversion is particularly efficient around $T_{1/2}$, which happens to be the inflection point of the thermal spin-crossover, 214 K according to Fig. 1(a). On closer inspection this maximum is shifted to temperatures below $T_{1/2}$, and under present excitation conditions the thermal conversion is maximum around 160 K, where $\Delta X_{\mathrm{HS}}{}^{\mu s} \approx 0.15$. We discuss that point thoroughly in Sec. IV.

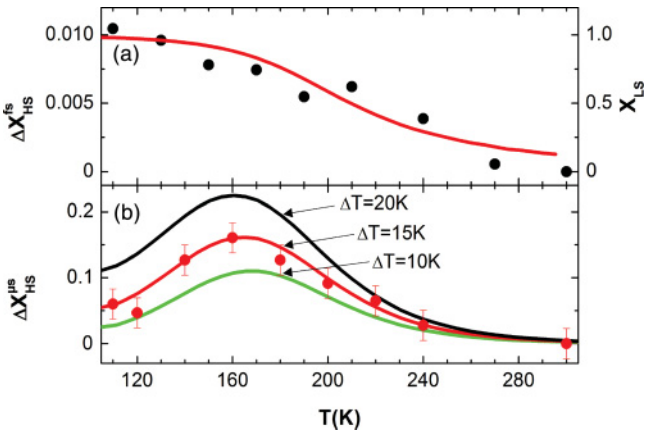

FIG. 5. (Color online) (a) Temperature dependence of the laser switched molecular fraction, $\Delta X_{\mathrm{HS}}{}^{fs}$ (dots), compared to X_{LS} (solid line). (b) Temperature dependence of the molecular fraction switched during microsecond step, $\Delta X_{\mathrm{HS}}{}^{\mu s}$ (dots), compared to the model of thermal conversion due to laser heating (solid lines). The model calculations were performed at three different values of temperature increase, $\Delta T = 10$ K, 15 K, 20 K. The corresponding calculated $\Delta X_{\mathrm{HS}}{}^{\mu s}$ at 180 K are pointed to with arrows.

IV. DISCUSSION ON SWITCHING DYNAMICS

Owing to satisfactory transient signal of the pump-probe optical experiments, three transformation steps are clearly distinguished during the switching dynamics. This agrees with three steps revealed by time-resolved x-ray diffraction study[18] on the same timescale. A major new feature is the significant increase of switched molecules during the elastic step. In addition, the temperature dependencies of the switched molecular fraction on picoseconds and microsecond timescales are different (Fig. 5). We discuss hereafter the nature of the elastic step as well as the origin of the difference just mentioned.

A. Femtosecond photoinduced switching step

According to Fig. 5(a), $\Delta X_{\mathrm{HS}}{}^{fs}$ decreases when temperature increases. This behavior follows rather closely that of the temperature dependence of the LS fraction X_{LS} ($= 1 - X_{\mathrm{HS}}$), which suggests that the earliest step of the spin switching occurs only on those LS molecules that absorbed pump-laser photons. The LS molecules thus promoted at $t = 0$ to the FC state will not necessarily all relax to the HS state, as different relaxation pathways are possible quantum mechanically, and the efficiency of a given pathway will depend on the oscillator strength between transient states. Notwithstanding possibly complex ultrafast pathway, the fraction of laser switched HS molecules is simply proportional to $X_{\mathrm{LS}}(T)$. This result implies that intramolecular processes are solely responsible for the physics of spin switching on the ultrashort timescale.

The switching efficiency at long times, funneling all processes, appears less intuitive and requires a closer look. We discuss the relevant dynamics in the following sections.

B. Nanosecond elastic step

The importance of elastic effects during spin-crossover transformations has already been pointed to, and a fair amount of experimental[4] and theoretical work dedicated to this problem.[24–26] Different molecular volumes in LS and HS states, the latter determined bigger,[6,19] underpin the elastic nature of cooperative interactions between molecules. The energy released by molecules relaxing from the excited states is nonradiatively dissipated during the previous step. Because

of the swelling of laser switched molecules and heating of the lattice, the crystal will expand. However, the volume expansion is not instantaneous because it involves propagation over relatively long distances, typically the crystal dimensions. Thus, the first step occurs at constant volume and results in the increase of pressure. During the second step, the volume expands allowing relaxation of pressure. This process involves a nonlinear propagation of the pressure front over macroscopic dimensions, in a shockwave-like fashion, whose dynamics are limited by a velocity similar to the sound velocity in solids.[23] Propagation of volume expansion in real-time was also demonstrated in liquids with picosecond x-ray pulses.[27] Given the crystal size, this sets the typical timescale to a few nanoseconds, in agreement with Fig. 3(b). The first act of pressure is a compression front trailing in its wake a depression. The latter leaves space for the molecules to swell and so to switch from LS to HS states. Both the volume expansion and the increase of HS molecular fraction during this elastic step are consequences of the same cause: the propagating pressure front. We note that the temperature evolution of $\Delta I/I$ at the nanosecond and microsecond steps bear very close resemblance, and both show maximum at 160 K (Fig. 4). We emphasize that the present collective response in the dynamical out-of-equilibrium process, leading to self-amplified switching, propagates with a typical velocity of a few km/s. This is very fast compared to the phase front propagation during the thermal transformation whose dynamics in similar systems are reported to be in the μm/s range.[28] The role of such nonlinear waves[29–31] is a current topic of interest in condensed matter. We demonstrate here that they can drive the spin-switching in a macroscopic solid in less than 100 ns under present experimental conditions.

C. Microsecond thermal step

The results presented in Sec. III C and those already discussed in the literature,[11,12,18] support the occurrence of significant thermal switching at the microsecond timescale. In order to explain the temperature dependence of $\Delta X_{\mathrm{HS}}{}^{\mu s}$, we test a model based primarily on the temperature dependencies of heat capacity, C_p, and X_{LS}. We start by evaluating the amount of energy, E_a, deposited on the crystal by the laser pump. Because the energy, E, contained in the laser pulse is mainly absorbed by the LS molecules, as explained in Sec. IV A, the following simple proportionality holds for our evaluation:

$$E_a \propto X_{\mathrm{LS}} \times E. \tag{7}$$

Most of E_a is redistributed over internal vibration modes and phonons during the relaxation process from the LMCT states to the lower lying HS state. Thus generated heat will diffuse on a timescale determined by diffusivity (typically 10^{-6} $\mathrm{m^2\,s^{-1}}$) causing temperature increase, ΔT, on the macroscopic scale of the crystal. The following expression relates C_p to E_a:

$$E_a(T) = \int_T^{T+\Delta T} C_p(T)dT. \tag{8}$$

By comparing Eqs. (7) and (8) and assuming a small temperature increase ΔT, the following is justified:

$$E_a(T) = C_p(T) \times \Delta T = A \times X_{\mathrm{LS}}(T), \tag{9}$$

where A factors in all temperature-independent quantities, including E. Thus far the temperature dependence of ΔT has not been explicit. Furthermore, Eq. (9) prompts the way for determining ΔT, namely,

$$\Delta T = A \times X_{\mathrm{LS}}(T)/C_p(T). \tag{10}$$

This ΔT will cause on the microsecond timescale X_{HS} to increase by $\Delta X_{\mathrm{HS}}{}^{\mu s}(T)$, where

$$\begin{aligned}\Delta X_{\mathrm{HS}}^{\mu s}(T) &= X_{\mathrm{HS}}(T+\Delta T) - X_{\mathrm{HS}}(T) \\ &= X_{\mathrm{HS}}(T + A \times X_{\mathrm{LS}}(T)/C_p(T)) - X_{\mathrm{HS}}(T).\end{aligned} \tag{11}$$

The temperature dependence of $\Delta X_{\mathrm{HS}}{}^{\mu s}$ can be straightforwardly determined from Eq. (11), as the temperature dependencies of C_p, X_{LS}, and X_{HS} are known from experiment (Fig. 1). For a quantitative discussion we calculated $\Delta X_{\mathrm{HS}}{}^{\mu s}(T)$ for three values of A, each causing different ΔT. It follows from Eq. (10) that ΔT depends on the initial temperature T, whereas A can be scaled against ΔT at just one reference temperature. We arbitrarily chose the latter at 180 K, where we supposed ΔT of 10 K, 15 K, and 20 K. The corresponding $\Delta X_{\mathrm{HS}}{}^{\mu s}(T)$ are plotted in Fig. 5(b). The best match to $\Delta X_{\mathrm{HS}}{}^{\mu s}(T)$ observed in the experiment is obtained with A scaled to ΔT of 15 K. With such A, $\Delta X_{\mathrm{HS}}{}^{\mu s}$ should peak at 165 K with a value of 0.15, both of which agree with the experiment. The time-resolved x-ray diffraction experiment,[23] carried out under comparable excitation conditions so that A is similar, yielded $\Delta X_{\mathrm{HS}}{}^{\mu s} \approx 0.1$ at 180 K, which too agrees with our model calculation.

This model, developed to describe the out-of-equilibrium thermo-switching, also explains why the maximum of $\Delta X_{\mathrm{HS}}{}^{\mu s}$ does not occur at $T_{1/2}$, as could be intuitively suspected. Figure 1(a) shows schematically that the same laser pump energy, E, induces different temperature increase, ΔT_1 and ΔT_2, depending on the initial temperature. Moreover, despite the fact that $T_1 < T_2$, the overall temperature effect can be opposite, $\Delta T_1 > \Delta T_2$. Such behavior is a consequence of counteracting contributions from X_{LS}, decreasing with temperature, and $C_p(T)$, increasing with temperature. Therefore, the magnitude of the thermal switch at T_1, equal to $\Delta X_{\mathrm{HS1}}{}^{\mu s}$, can be greater than $\Delta X_{\mathrm{HS2}}{}^{\mu s}$ at T_2. Increasing E magnifies the effect, as ΔT is greater, and Fig. 5(b) reveals this trend, too.

A hypothesized limit for $\Delta X_{\mathrm{HS}}{}^{\mu s}$ is hard to verify experimentally, as lowering the temperature prolongs the lifetime of photoexcited HS molecules,[8] up to a point where the lifetime becomes longer than the period of laser excitation. In addition, increasing E causes crystal damage. For circumventing these limitations time-resolved single-shot experiments hold big promise, and the first attempts have proven successful in diverse applications utilizing single pulse of laser,[32] x rays,[33] or electrons.[34,35]

V. CONCLUSIONS

In this report we have monitored the optical transmission of an Fe(III) crystal following spin-crossover triggered by ultra-short light pulse. In particular, by synchronizing two laser amplifiers we extend our earlier studies on the ultrafast timescale to the time domains associated with elastic propagation and heat diffusion across the crystal. We emphasize that the transformation pathway is multistep. At first, the laser pulse initiates purely photoinduced increase of X_{HS}, complete within 300 fs. Then, every photoexcited molecule releases heat through electron-phonon and vibronic relaxations, which trigger local amplification as the energy converted from photon spreads over neighboring molecules. Local thermalization, constrained to constant volume, settles rapidly in less than 1 ns. It is ensued by volume expansion, with amplification through elastic interactions, and finally thermal activation and heat diffusion throughout the sample. These slower processes increase both X_{HS} and the unit cell volume. The thermal equilibrium is recovered within 1 ms. Efforts are underway to drive photoinduced transitions in highly cooperative systems,[9,10] for which the out-of-equilibrium dynamics may be different. Investigations of photoactive and thermoactive materials on nanosecond to microsecond timescales underline the role of elastic and laser-heating effects and open perspectives for such investigations inside thermal hysteresis.[9–11]

New experiments will have to be devised, whereby coherent elastic switching can be observed and controlled.[36] In addition, the new generation of ultrafast structural experiments will provide a great input owing to such possibilities as capturing local clustering[37] or shock-wave effects.[31] Finally, the role of elastic-driven transition in a bi-stable molecular system needs to be further investigated from the theoretical view point. Until now, the different models developed discussed the important role of elastic effects at the microscopic level.[4,24–26] But the present results, on fast and ultra-fast transformation of matter with light, clearly evidence that macroscopic descriptions are required, with shock-wave driven transformation taken into account. The present study also offers clues for designing efficient photoactive devices by taking advantage of thermal and elastic effects. Systems with low C_p will allow attaining greater temperature increase during thermal switching, whereas systems with stronger elastic coupling and smaller size, such as nano-particles, will allow faster and more efficient elastic switching.

ACKNOWLEDGMENTS

This work was supported by the Institut Universitaire de France, Rennes Métropole, Région Bretagne (CREATE Ultimate 4146), the ANR (09BLAN-0212), and Europe (FEDER). CB thanks the Région Bretagne for PD funding. WK thanks IUF, UR1 for covering part of his Ph.D. grant. We thank Aleksandra Pajzderska for help in DSC measurements.

*To whom correspondence should be addressed: maciej.lorenc@univ-rennes1.fr

†Current address: Laboratoire de Chimie et Physique des Matériaux (LCPM) Université de Ziguinchor, Bp: 523 Ziguinchor, Sénégal.

[1] M. Rini, R. Tobey, N. Dean, J. Itatani, Y. Tomioka, Y. Tokura, R. W. Schoenlein, and A. Cavalleri, Nature **449**, 72 (2007).

[2] M. Chollet, L. Guerin, N. Uchida, S. Fuhaya, H. Shimoda, T. Ishikawa, K. Matsuda, T. Hasegawa, A. Ota, H. Yamochi, G. Saito, R. Tazaki, S. Adachi, and S. Koshihara, Science **307**, 86 (2003).

[3] S. Koshihara and M. Kuwata-Gonokami, (eds.), J. Phys. Soc. Jpn. **75**, 011001 (2006).

[4] P. Gütlich and H. A. Goodwin, (eds.), Top. Curr. Chem. **233-235** (2004).

[5] J. F. Létard, L. Capes, G. Chastanet, N. Moliner, S. Létard, J. A. Real, and O. Kahn, Chem. Phys. Lett. **313**, 115 (1999).

[6] E. Collet, M. Buron-Le Cointe, and H. Cailleau, J. Phys. Soc. Jpn. **75**, 011002 (2006).

[7] N. Bréfuel, H. Watanabe, L. Toupet, J. Come, N. Matsumoto, E. Collet, K. Tanaka, and J.-P. Tuchagues, Angew. Chem. Int. Ed. **48**, 9304 (2009).

[8] C. Enachescu, A. Hauser, J.-J. Girerd, and M.-L. Boillot, Chem. Phys. Chem. **7**, 1127 (2006).

[9] E. Freysz, S. Montant, S. Létard, and J.-F. Létard, Chem. Phys. Lett. **394**, 318 (2004).

[10] S. Bonhommeau, G. Molnar, A. Galet, A. Zwick, J.-A. Real, J. J. McGarvey, and A. Bousseksou, Angew. Chem. Int. Ed. **44**, 4069 (2005).

[11] O. Fouché, J. Degert, G. Jonusauskas, N. Daro, J.-F. Létard, and E. Freysz, Phys. Chem. Chem. Phys. **12**, 3044 (2010).

[12] G. Galle, J. Degert, C. Mauriac, C. Etrillard, J. F. Letard, and E. Freysz, Chem. Phys. Lett. **500**, 18 (2010).

[13] W. Gawelda, V.-T. Pham, M. Benfatto, Y. Zaushitsyn, M. Kaiser, D. Grolimund, S. L. Johnson, R. Abela, A. Hauser, C. Bressler, and M. Chergui, Phys. Rev. Lett. **98**, 057401 (2007).

[14] C. Bressler, C. Milne, V.-T. Pham, A. El Nahhas, R. M. van der Veen, W. Gawelda, S. Johnson, P. Beaud, D. Grolimund, M. Kaiser, C. N. Borca, G. Ingold, R. Abela, and M. Chergui, Science **323**, 489 (2009).

[15] M. Khalil, M. M. Marcus, A. L. Smeigh, J. K. McCusker, H. H. W. Chong, and R. W. Schoenlein, J. Phys. Chem. A **110**, 38 (2006).

[16] C. Brady, J. J. McGarvey, J. K. McCusker, H. Toftlund, and D. N. Hendrickson, Top. Curr. Chem. **235**, 1 (2004).

[17] A. Cannizzo, F. van Mourik, W. Gawelda, G. Zgrablic, C. Bressler, and M. Chergui, Angew. Chem. Int. Ed. **45**, 3174 (2006).

[18] M. Lorenc, J. Hébert, N. Moisan, E. Trzop, M. Servol, M. Buron-Le Cointe, H. Cailleau, M.-L. Boillot, E. Pontecorvo, M. Wulff, S. Koshihara, and E. Collet, Phys. Rev. Lett. **103**, 028301 (2009).

[19] E. Collet, M.-L. Boillot, J. Hébert, N. Moisan, M. Servol, M. Lorenc, L. Toupet, M. Buron-Le Cointe, A. Tissot, and J. Sainton, Acta Cryst. **B65**, 474 (2009).

[20] T. Nakamoto, Z.-C. Tan, and M. Sorai, Inorg. Chem. **40**, 3805 (2001).

[21]N. Moisan, M. Servol, M. Lorenc, A. Tissot, M.-L. Boillot, H. Cailleau, S. Koshihara, and E. Collet, C. R. Chimie **11**, 1235 (2008).
[22]D. Boschetto, E. G. Gamaly, A. V. Rode, B. Luther-Davies, D. Glijer, T. Garl, O. Albert, A. Rousse, and J. Etchepare, Phys. Rev. Lett. **100**, 027404 (2008).
[23]H. Cailleau, M. Lorenc, L. Guérin, M. Servol, E. Collet, and M. Buron-Le Cointe, Acta Cryst. **A66**, 189 (2010).
[24]H. Spiering, Top. Curr. Chem. **235**, 171 (2004).
[25]M. Nishino, K. Boukheddaden, Y. Konishi, and S. Miyashita, Phys. Rev. Lett. **98**, 247203 (2007).
[26]N. Nagaosa and T. Ogawa, Phys. Rev. B **39**, 4472 (1999).
[27]M. Wulff, S. Bratos, A. Plech, V. Vuilleumier, F. Mirloup, M. Lorenc, Q. Kong, and H. Ihee, J. Chem. Phys. **124**, 034501 (2006).
[28]C. Chong, A. Slimani, F. Varret, K. Boukheddaden, E. Collet, J.-C. Ameline, R. Bronisz, and A. Hauser, Chem. Phys. Lett. **504**, 29 (2011).
[29]P. Babilotte, P. Ruello, D. Mounier, T. Pezeril, G. Vaudel, M. Edely, J.-M. Breteau, V. Gusev, and K. Blary, Phys. Rev. B **81**, 245207 (2010).
[30]Y. Okimoto, M. Kurashima, K. Seko, T. Ishikawa, K. Onda, S. Koshihara, T. Kyomen, and M. Itoh, Phys. Rev. B **83**, 161101 (2011).
[31]D. H. Kalantar, J. F. Belak, G. W. Collins, J. D. Colvin, H. M. Davies, J. H. Eggert, T. C. Germann, J. Hawreliak, B. L. Holian, K. Kadau, P. S. Lomdahl, H. E. Lorenzana, M. A. Meyers, K. Rosolankova, M. S. Schneider, J. Sheppard, J. S. Stölken, and J. S. Wark, Phys. Rev. Lett. **95**, 075502 (2005).
[32]P. R. Poulin and K. A. Nelson, Science **313**, 1756 (2006).
[33]A. M. Lindenberg, J. Larsson, K. Sokolowski-Tinten, K. J. Gaffney, C. Blome, O. Synnergren, J. Sheppard, C. Caleman, A. G. MacPhee, D. Weinstein, D. P. Lowney, T. K. Allison, T. Matthews, R. W. Falcone, A. L. Cavalieri, D. M. Fritz, S. H. Lee, P. H. Bucksbaum, D. A. Reis, J. Rudati, P. H. Fuoss, C. C. Kao, D. P. Siddons, R. Pahl, J. Als-Nielsen, S. Duesterer, R. Ischebeck, H. Schlarb, H. Schulte-Schrepping, Th. Tschentscher, J. Schneider, D. von der Linde, O. Hignette, F. Sette, H. N. Chapman, R. W. Lee, T. N. Hansen, S. Techert, J. S. Wark, M. Bergh, G. Huldt, D. van der Spoel, N. Timneanu, J. Hajdu, R. A. Akre, E. Bong, P. Krejcik, J. Arthur, S. Brennan, K. Luening, and J. B. Hastings, Science **308**, 392 (2005).
[34]P. Musumeci, J. T. Moody, C. M. Scoby, M. S. Gutierrez, H. A. Bender, and N. S. Wilcox, Rev. Sci. Instrum. **81**, 013306 (2010).
[35]R. Li, W. Huang, Y. Du, L. Yan, Q. Du, J. Shi, J. Hua, H. Chen, T. Du, H. Xu, and C. Tang, Rev. Sci. Instr. **81**, 036110 (2010).
[36]T. Feurer, J. C. Vaughan, and K. A. Nelson, Science **299**, 374 (2003).
[37]L. Guérin, J. Hébert, M. Buron-Le Cointe, S. I. Adachi, S. Y. Koshihara, H. Cailleau, and E. Collet, Phys. Rev. Lett. **105**, 246101 (2010).